JOC The Journal of Organic Chemistry

Article

pubs.acs.org/joc

Reaction Mechanism of an Intramolecular Oxime Transfer Reaction: A Computational Study

Jani Moilanen,* Antti Neuvonen, and Petri Pihko*

Department of Chemistry, University of Jyväskylä, P.O. Box 35, FI-40014 Jyväskylä, Finland

Supporting Information

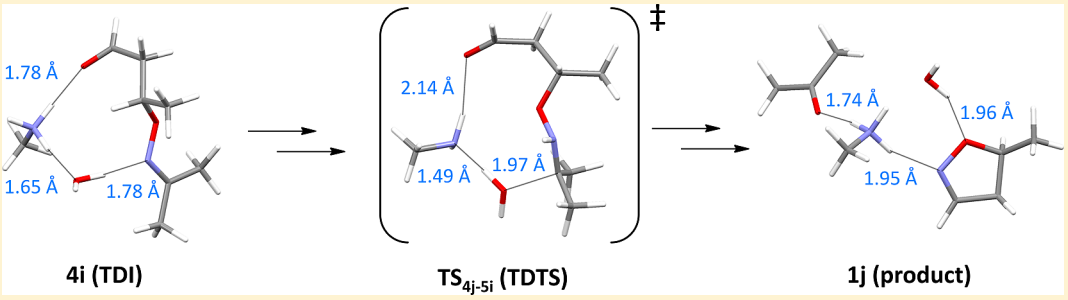

ABSTRACT: Density functional theory (PBE0/def2-TZVPP) calculations in conjunction with a polarizable continuum model were used to assess the mechanism of the intramolecular oxime transfer reaction that leads to the formation of isoxazolines. Different diastereomers of the intermediates as well as different oximes (formaldehyde and acetone oxime) were considered. The computed reaction profile predicts the water-addition and -expulsion steps as the highest barriers along the pathway, a conclusion that is in line with the experimental evidence obtained previously for these reactions.

INTRODUCTION

Gathering evidence for a proposed reaction mechanism involving several reactive intermediates and complex equilibria can be challenging, even with modern spectroscopic methods and kinetic experiments. The main difficulty arises when the intermediates escape experimental detection and identification. In these cases, the use of computational methods should give further insights into the plausibility of the mechanism and the relative stabilities of postulated short-lived intermediates. Herein, we discuss a case involving a seemingly simple oxime transfer reaction where the key intermediates could not be detected experimentally and a tentative mechanism was inferred from substituent effects.

We have previously reported both racemic and enantioselective organocatalytic methods for the synthesis of 3-unsubstituted 2-isoxazolines (**1**) from oximes (**2**) and α,β-unsaturated aldehydes (**3**).[1] In conjunction with these studies, the mechanism of this transformation has been studied by kinetic measurements and analysis of the product distributions, leading to the following observations on the mechanism.[1b] NMR monitoring of the reaction progress indicated that the reaction likely proceeds via conjugate addition product **4** because the concentration of this intermediate climbs and falls during the initial stages of the reaction and the concentration of isoxazoline then starts to increase. Evidence for the iminium catalysis of this step can be obtained from the observed sense of enantioselection when the reaction was carried out with chiral amines[1b] (Scheme 1), and as such, the mechanistically more intriguing transformation was the transformation of **4** to **1**. For this step, the experimental evidence was inconclusive.

Experimentally, this step was examined by NMR with separately prepared conjugate addition product **4**, and these studies established that this sequence was likely to be acid-catalyzed and not iminium-catalyzed. Faster rates were obtained with acids such as diphenyl phosphate than with the corresponding ammonium salts (e.g., *N*-methylammonium diphenyl phosphate). Further investigations of the entire reaction sequence suggested that increasing the concentration of water in the reaction medium increased the rate slightly, whereas a further substitution in the β position of enal **3** led to more significant increases in the overall rate and concomitant decrease in the peak concentration of intermediate **4**. Furthermore, cyclohexanone oxime turned out to be superior to both acetone oxime as well as cyclopentanone oxime in terms of rate. If the reaction proceeds via tetrahedral intermediates **5**−**7** (Scheme 2), then the results with different oximes suggest that the most likely candidates for the rate-determining states are either connected to the first step (addition of H_2O) or the last step (expulsion of water and subsequent deprotonation). The faster rates obtained with β,β-disubstituted enals seemed to rule out the first possibility because the β substituents were unlikely to increase the rate of addition of H_2O to the oxime. These considerations suggested that the last step of the sequence (**7** → **1**, Scheme 2) involves the most likely candidate for the rate-determining states. However, the possibility that the reaction proceeds via an alternative pathway, where the expulsion of the carbonyl

Received: December 3, 2013
Published: February 11, 2014

dx.doi.org/10.1021/jo402676z | J. Org. Chem. 2014, 79, 2006−2014

Scheme 1. Previously Reported Organocatalytic Asymmetric Synthesis of 2-Unsubstituted Isoxazolines

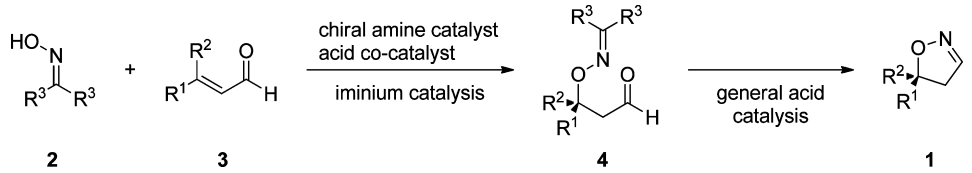

Scheme 2. Proposed Reaction Route for Isoxazoline Formation from Conjugate Addition Product 4

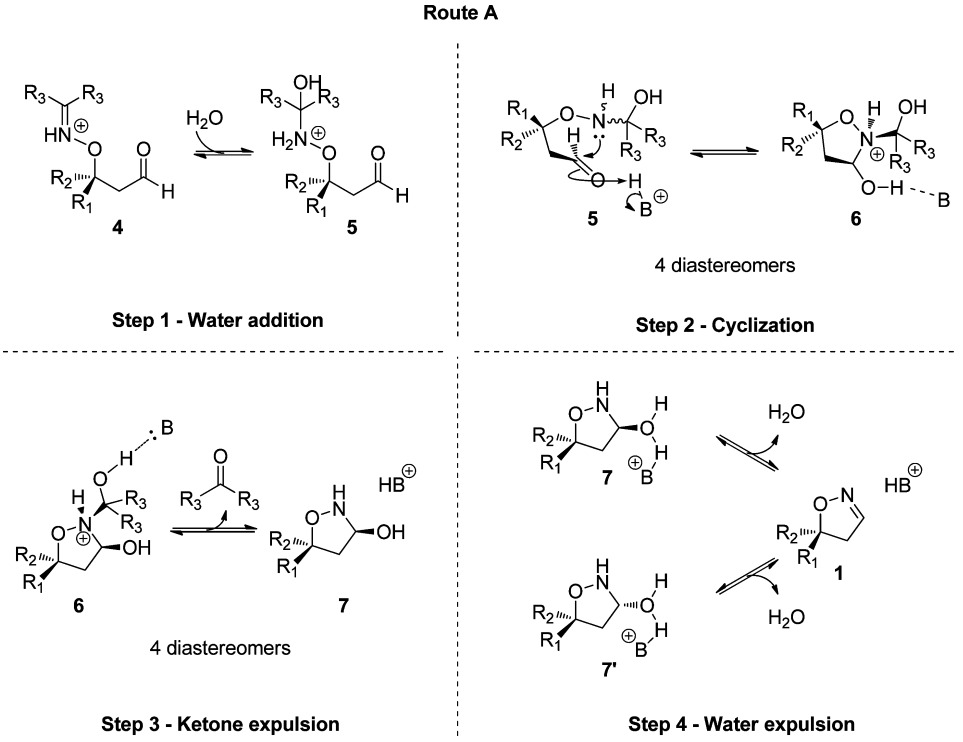

Scheme 3. Alternative Reaction Route for Isoxazoline Formation from Conjugate Addition Product 4

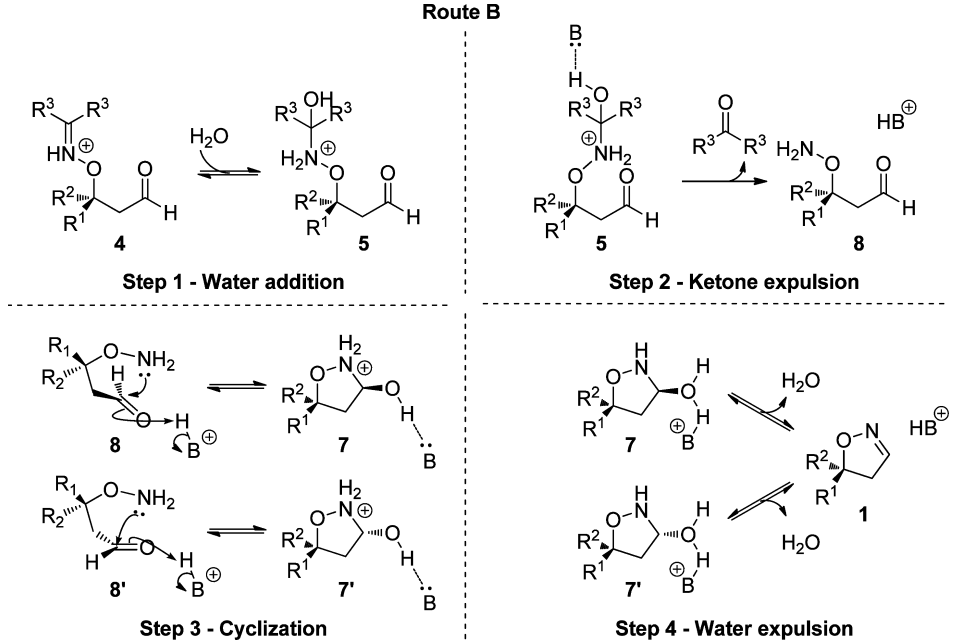

compound and cyclization take place in the reverse order, could not be excluded (Scheme 3).

If the reaction occurs via route A, then the oxime transfer reaction is likely initiated by the water-addition step in which

dx.doi.org/10.1021/jo402676z | J. Org. Chem. 2014, 79, 2006−2014

the water molecule attacks the oxime group of conjugate addition product **4**. Because the conjugate addition product is an observable intermediate (and thus reasonably stable), it can be assumed that the water-addition step is slow without proper catalysis. Indeed, the importance of acid catalysis in the reversible addition of water to oximes has been shown in extensive mechanistic studies that were carried out in aqueous media and at various pH values.[2] Moreover, as mentioned above, the oxime transfer reaction takes place in the presence of an acid catalyst also in nonpolar aprotic solvents. The role of the acid catalysis in aqueous[3a−c] and aprotic media[3d] has also been verified in computational studies. On the basis of these previous results, a reasonable first guess for the mechanism involves the reversible addition of water to the conjugate addition product under acid catalysis. We are aware that the nucleophile could also be another species, such as another oxime, but here we consider water as the first choice of the nucleophile.

The addition of water should lead to tetrahedral carbinolamine intermediate **5.** It is expected that the nitrogen in the carbinolamine is more nucleophilic than the nitrogen in oxime species **4**; thus, an acid-catalyzed intramolecular 1,2-addition to aldehyde can proceed after the water-addition step.[4]

Because the cyclization step yields a new carbinolamine, **6**, with additional stereocenters at nitrogen and C3, it is plausible that the cyclization step gives a mixture of diastereoisomers that lead to competitive reaction routes. Despite the effort, no diastereomeric intermediates **6** could be detected by ^{1}H NMR or trapped by silylation in previous experimental studies, indicating that the carbinolamine diastereomers are highly reactive intermediates within the reaction. Because the carbinolamine stereocenters are lost after the water elimination step, the gathered experimental data provide no indication that one diastereomeric route is favored over the others.[1b]

After the cyclization step, the expulsion of carbonyl compound can take place. This step is considered to be catalyzed by the conjugate base generated in the previous step. In addition to deprotonation of the forming oxonium ion, this step requires activation of the carbinolamine nitrogen by protonation. Sayer and co-workers found that both of these factors affect the rate of the reversible formation of tetrahedral carbinolamine products in acidic aqueous solutions.[4b] In addition, they concluded that the formation of a zwitterionic ammonium−alkoxide intermediate leads to a rapid collapse of the carbinolamine to an amine and a carbonyl species.

The final step of the oxime transfer reaction is the water expulsion that is comparable to the dehydration step of oxime formation reactions. Under aqueous and neutral conditions, the dehydration of the oxime is the rate-determining step and the observed kinetic isotope effect is consistent with general acid catalysis.[4a] As a consequence, it is highly likely that the proton transfer or hydrogen-bond activation of the hydroxyl group of intermediate **7** catalyzes the water expulsion, which yields a protonated isoxazoline species. Final deprotonation affords the desired 2-isoxazoline product.

In route B, the steps of route A are traced in reverse order. Therefore, the above reaction mechanism discussion is also applicable to route B. However, if the cyclization step is reasonably fast, then route A will be a more possible route for the intramolecular oxime transfer reaction.[1b]

The purpose of the present study is to examine these reaction routes and steps in more detail and to find out the most plausible reaction mechanism for the intramolecular oxime transfer reaction using DFT calculations. First, we briefly discuss our computational model systems. Second, we investigate the mechanism and the thermochemistry of the cyclization, carbonyl-expulsion, and water-expulsion steps (steps 2−4 in Schemes 2 and 3) of the oxime transfer reaction by means of the simple model systems (formaldehyde oxime models). Third, we study the whole reaction pathway using a more realistic system, a ketone oxime (acetone oxime model), and last, we compare experimental and computational data. Given the complexity of the possible reaction pathway and the possibility of several different diastereomeric intermediates, studying the effect of different R^1 and R^2 substituents is omitted from the calculations.

■ COMPUTATIONAL DETAILS

All calculations were performed employing the PBE0 hybrid-exchange correlation functional in conjunction with improved default triple-ζ valence-polarized basis set, namely, def2-TZVPP, in solution phase.[5,6] The presence of solvent was taken into account using the integral equation formalism variant of the polarizable continuum model employing toluene as a solvent.[7]

The potential energy surface (PES) scans with respect to the selected internal reaction coordinate followed by full geometry optimizations were carried out to obtain the transition states. For each optimized transition state, the intrinsic reaction coordinate (IRC) calculation was performed to acquire starting geometries for reactants and products by following the reaction path along the transition vector to both directions.[8] Subsequent geometry optimizations were carried out for initial structures obtained from IRC calculations to find minimum structures for each intermediate. In all calculations, several different conformers were tested to locate the lowest-energy minima and transition states on the potential energy hypersurface.

Frequency analyses were performed for all stationary points found to ensure that they correspond to either true minima (no imaginary frequencies) or first-order transition states (only one negative imaginary frequency). The thermochemical data were acquired at T = 298.15 K and P = 101.325 kPa (1 atm) using the ideal gas−rigid rotor−harmonic oscillator approximation as implemented in Gaussian09.[9]

To find out the rate-determining states for the intramolecular oxime transfer reaction, we used the energetic span concept as defined by Kozuch and Shaik.[10] In this terminology, the efficiency of the catalytic cycle (i.e., the turnover frequency, TOF) is determined by one transition state and one intermediate, which are called the TOF-determining transition state (TDTS) and TOF-determining intermediate (TDI).

All calculations were performed with Gaussian 09,[9] whereas the visualizations of compounds were done with Mercury.[11]

■ RESULTS AND DISCUSSION

To the best of our knowledge, no previous computational studies have been reported for the either inter- or intramolecular oxime transfer reactions in the literature. Only a handful of similar computational and theoretical investigations have been published, but they have mainly concentrated on the hydrolysis and isomerization of oximes.[3] Hence, it was necessary to obtain a preliminary picture from the oxime transfer reaction by computational investigation of a simpler formaldehyde oxime model systems (R^1 = R^3 = H, R^2 = Me) before performing calculations with the larger and more realistic acetone oxime model (R^1 = H, R^2 = R^3 = Me).[5,6] The solvent effect was included in the calculations because all experimental reactions have been done in nonpolar and aprotic solvents and because it has been shown in numerous studies that the presence of the solvent influences the reaction energy profile.[12] Although both model systems investigated in this

dx.doi.org/10.1021/jo402676z | J. Org. Chem. 2014, 79, 2006−2014

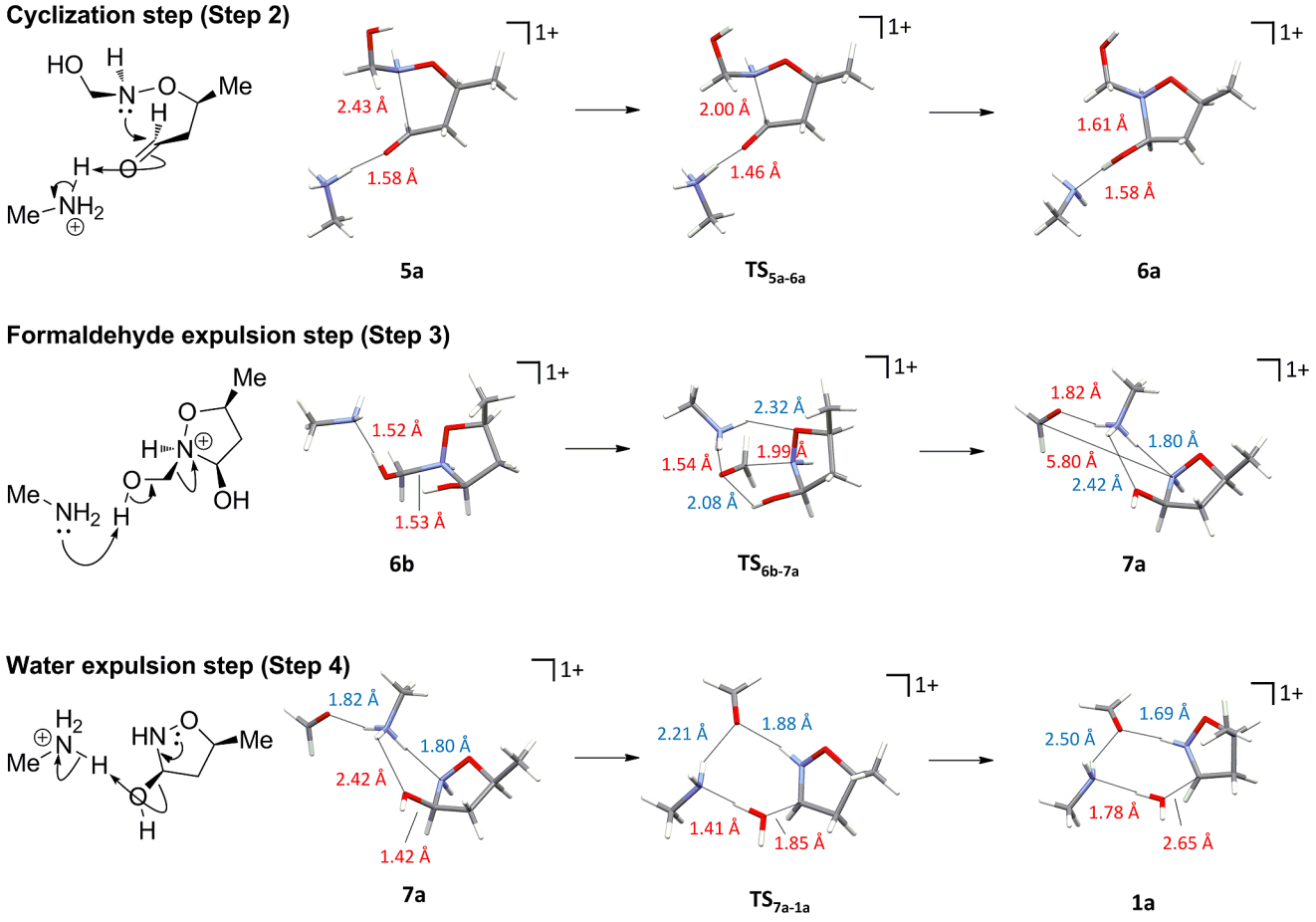

Figure 1. Optimized geometries of reactants, transition states, and products for the first (2*R**,3*R**,5*S**) diastereomer series (isoxazolidine numbering) of the formaldehyde oxime model. Color code: red = reaction coordinate, and blue = hydrogen bond. Schematic mechanisms are also included for each step. The optimized geometries of three other diastereomers are presented in the Supporting Information (Figures S1–S3).

study are simplified if compared to the experimental setting, they were further simplified to lower the computational cost of calculations by omitting the weakly coordinating anion, such as the diphenylphosphate anion.

In analogy to the experimental studies on oxime formation and hydrolysis,[2,4] the reaction pathway of the present oxime transfer reaction can be considered to include general acid- or base-catalyzed steps that involve synchronous or rapid proton transfers. Because our previous experimental mechanistic studies on this reaction were carried out under moderately acidic conditions (oxoacids or their ammonium salts[1]), methylammonium ion and its conjugate base methylamine were selected as the acid and base catalysts, respectively, for the computational studies. In addition to this, the proposed intermediates have functionalities that can act as H-bond donors or acceptors. Therefore, it was crucial to use a quantum chemical method capable of describing hydrogen bonding and to ensure that the energy differences between diastereomeric routes do not arise solely from different hydrogen-bond networks of optimized complexes.[13]

Reaction Mechanism. The computational examination of the oxime transfer reaction was started from route A and from the cyclization step using four formaldehyde oxime models, **5a**–**5a‴**. Calculations reveal that the transition states $\mathbf{TS_{5a-6a}}$–$\mathbf{TS_{5a‴-6a‴}}$ involve a synchronized formation of a C–N single bond and a proton transfer from methylammonium to the aldehyde oxygen (Figures 1 and S1–S3). That is, the cyclization occurs in a concerted manner. Following the transition vectors of transition states $\mathbf{TS_{5a-6a}}$–$\mathbf{TS_{5a‴-6a‴}}$ in the forward direction leads to the closure of the five-membered ring in each case and the formation of four diastereomer,s **6a**–**6a‴**, with stereocenters at nitrogen, C3, and C5 (2-isoxazoline numbering).[14] In the product complex, methylamine is hydrogen-bonded to all diastereomers in a similar manner.

The aldehyde-expulsion step begins with the structural reorganization of hydrogen-bonded complexes of **6a**–**6a‴**, giving four new complexes, **6b**–**6b‴**, respectively, in which methylamine forms a new hydrogen bond with the hydroxyl group of the carbinolamine group (Figures 1 and S1–S3). This reorganization ensures that methylamine can act as a base catalyst in the aldehyde-expulsion step. After the reorganization, the aldehyde-expulsion step proceeds in a concerted manner like the cyclization step: transition states $\mathbf{TS_{6b-7a}}$–$\mathbf{TS_{6b‴-7a‴}}$ involve a proton transfer from carbinolamine to methylamine in conjunction with C–N single bond breaking between the expulsing formaldehyde and ring system. As a consequence, four hydrogen-bond complexes, **7a**–**7a‴**, are formed. Although the hydrogen-bond complexes of **6b**–**6b‴** and **7a**–**7a‴** are quite identical, small variations can be seen in transition states ($\mathbf{TS_{6b-7a}}$ and $\mathbf{TS_{6b′-7a′}}$ vs $\mathbf{TS_{6b″-7a″}}$ and $\mathbf{TS_{6b‴-7a‴}}$) because of the different orientation of the hydroxyl group of the isoxazolidine ring (Figures 1 and S1–S3).

The close spatial proximity of methylammonium ion and the hydroxyl group of the oxime in hydrogen-bond complexes **7a**

dx.doi.org/10.1021/jo402676z | J. Org. Chem. 2014, 79, 2006–2014

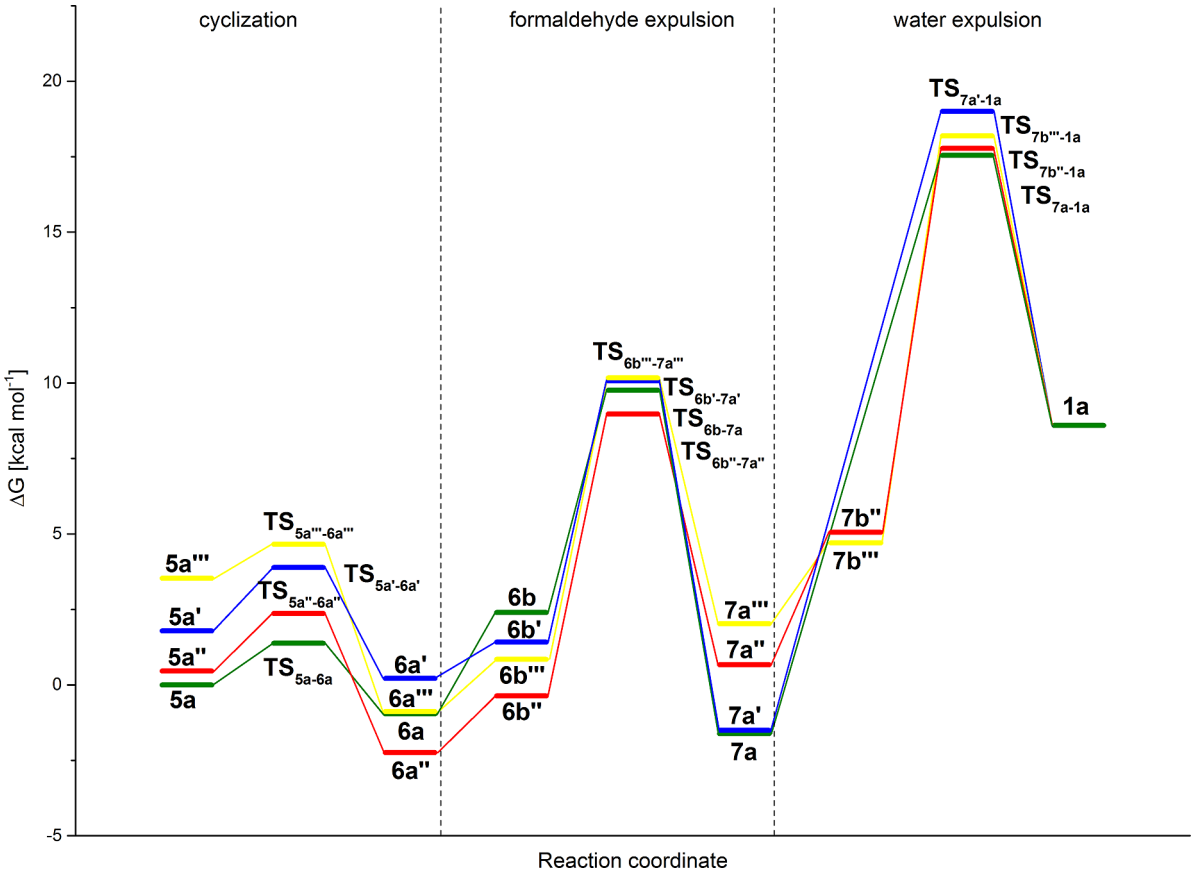

Figure 2. Calculated Gibbs free energies for formaldehyde oxime models: diastereomer 1 (green), diastereomer 2 (blue), diastereomer 3 (red), and diastereomer 4 (yellow). All values are scaled to the Gibbs free energy of **5a**, and they are also listed in Table S1.

and **7a**′ enables the last step of the oxime transfer reaction (the water-expulsion step) to proceed without significant reorganization of **7a** or **7a**′ (Figures 1 and S1). However, **7a**″ and **7a**‴ have to undergo reorganization to **7b**″ and **7b**‴ before the water-expulsion step can take place (see Supporting Information Figures S2 and S3). This reorganization also has an effect on the geometries of transition states $\mathbf{TS}_{\mathbf{7b''-1a}}$ and $\mathbf{TS}_{\mathbf{7b'''-1a}}$, which display dissimilar hydrogen-bonded complexes compared to $\mathbf{TS}_{\mathbf{7a-1a}}$ and $\mathbf{TS}_{\mathbf{7a'-1a}}$. Despite the different hydrogen-bond networks, the transition vectors of all transition states are connected to a proton transfer from methylammonium ion to the hydroxyl group of oxime and the breaking of O−C single bond of hydroxyl group. These processes are also evident from the structural changes (Figure 1), for example, the length of the O−C bond is 1.42, 1.85, and 2.65 Å in **7a**, $\mathbf{TS}_{\mathbf{7a-1a}}$, **1a**, respectively, indicating the clear elongation of O−C single bond during the reaction. IRC calculations for $\mathbf{TS}_{\mathbf{7a-1a}}$−$\mathbf{TS}_{\mathbf{7b'''-1a}}$ followed by geometry optimizations confirm that transition states lead to desired reaction product **1a**, of which a proton can be removed spontaneously in the presence of the base (see discussion below as well as Figure S4 and Table S2).[15]

For each step in route B, the conformations of the starting complex and the product were optimized, and transition states were searched. However, all PES scans with respect to the expulsion of the carbonyl compound from intermediate **5** led to higher-energy complexes. Also, no reasonable transition state could be found for this step. Thus, it is highly unlikely that the oxime transfer reaction takes place through reaction pathway B. Therefore, pathway B was excluded from further study.

Reaction Energy. Figure 2 shows computed Gibbs free energies for all formaldehyde oxime models. All acyclic intermediates, **5a**−**5a**‴, react with a methylammonium via a low-lying transition state to give cyclic intermediates **6a**−**6a**‴, respectively, which are lower in energy than the corresponding acyclic intermediates. This result indicates that the cyclization step of the reaction is exergonic and proceeds spontaneously. Even though the equilibrium of this step should be on the right side, it is feasible that the acyclic and cyclic intermediates are in a fast equilibrium because of their similar energies and small activation barriers between these species. The low activation barriers imply that diastereomers **6a**−**6a**‴ are all accessible and the overall significance of the cyclization step to the oxime transfer reaction is minor.

According to the proposed mechanism and calculations, methylamine participates in the aldehyde-expulsion step by general base catalysis and thus the expulsion of formaldehyde requires that methylamine coordinates to the proton of the formaldehyde carbinolamine. These changes in coordination (from **6a**−**6a**‴ to **6b**−**6b**‴) are slightly unfavorable with regard to free energy (Figure 2). The aldehyde-expulsion step has a higher activation barrier than the cyclization step: the activation energies of diastereomers vary between 1.0 and 2.1 kcal mol^{-1} in the cyclization step, whereas in the aldehyde-expulsion step, they are in the range of 9.9−11.2 kcal mol^{-1}.[16] This result and the fact that intermediates **7a**−**7a**‴ are clearly lower in energy than transition states $\mathbf{TS}_{\mathbf{7a-1a}}$−$\mathbf{TS}_{\mathbf{7b'''-1a}}$ indicate that the aldehyde-expulsion step is less reversible than the cyclization step.

dx.doi.org/10.1021/jo402676z | J. Org. Chem. 2014, 79, 2006−2014

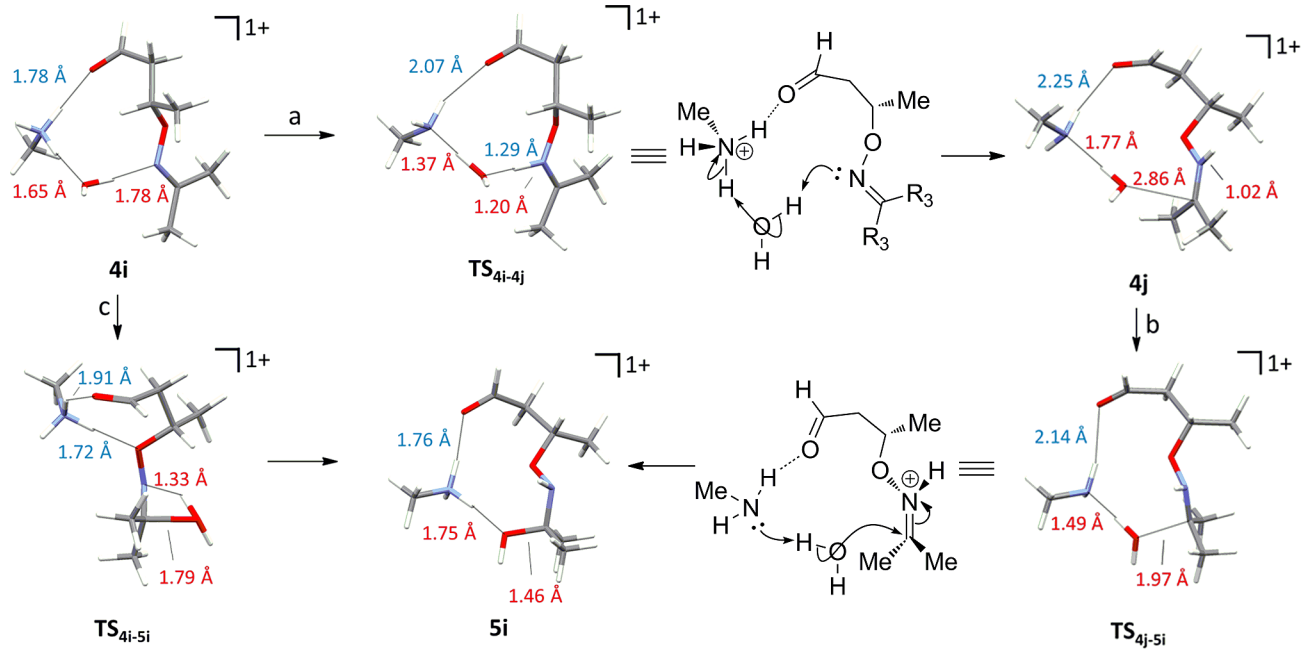

Figure 3. Calculated mechanisms via a stepwise (a, b) and concerted (c) pathway for the water-addition step in the acetone oxime model. Color code: red = reaction coordinate, and blue = hydrogen bond.

In the water-elimination step, the reorganization of hydrogen-bonded complex **7a**″ (**7a**‴) to **7b**″ (**7b**‴) is not energetically favorable (Figure 2) but was found to be necessary for this step to occur. Calculated transition states $\mathbf{TS_{7a-1a}}$–$\mathbf{TS_{7b'''-1a'''}}$ are global energy maxima for formaldehyde oxime models, suggesting that the TS of the water-expulsion step would be the TDTS in this case. As the stereocenters at nitrogen and carbon in position 3 are lost within the water-expulsion step, the transition states lay almost in same free energy on the potential energy surface and lead to protonated reaction product **1a.** Deprotonation of **1a** regenerates the catalyst and affords the final isoxazoline product as the global energy minimum for the whole reaction (see below).

The effect of the relative stereochemistry on the entire reaction pathway is small but nevertheless evident from the reaction energy data. For example, the similar hydrogen-bond networks in the cyclization step (**5a**–**5a**‴, **6a**–**6a**‴, and $\mathbf{TS_{5a-6a}}$–$\mathbf{TS_{5a'''-6a'''}}$) imply that the hydrogen bonding contributes little to the energy differences in this step (i.e., small energy differences between these hydrogen-bonded complexes arise from their different stereochemistry). In contrast, the energy differences between intermediates **7a**–**7a**‴ are affected more by the different configuration of functional groups because they cannot form identical H-bond networks.

Because the experimental data suggested that the water-expulsion step might be the rate-determining step, we decided to study this step in more detail by calculating the Gibbs free energy of the reaction under different conditions. More precisely, for the first diastereomer series (corresponding to the 2*S**,3*R**,5*S** relative stereochemistry, **5a**–**1a**), additional calculations were performed by varying the number of hydrogen bonds within the complex. In addition, the effect of changing the reaction conditions from acidic to basic was also studied (for more details, see Figure S4 in the Supporting Information).

To determine the importance of the number of hydrogen bonds in the complexes, the calculations for the water-expulsion step were performed starting from singly (**7c**) and doubly (**7d**) hydrogen-bonded intermediates. As expected, the doubly hydrogen-bonded complex is stabilized by the additional H-bond (~4.0 kcal mol^{-1}), but it has an unfavorable effect, although very small (~0.5 kcal mol^{-1}), on the transition-state energy. The energy difference could be explained by a higher entropic cost relative to the singly H-bonded starting complex and the loss of stabilization because of the weakened H-bond.

As the oxime formation from hydroxylamine and carbonyl compounds is known to be pH-sensitive in aqueous solutions[2a] and the oxime transfer step was highly dependent on the pK_{aH} of the amine catalyst (e.g., *N*-methylaniline versus pyrrolidine),[1b] we expected to see differences in the transition-state energies under acidic and basic conditions. Thus, the calculations for the isoxazoline formation from carbinolamine were also performed in the presence of 1 equiv of base: hydroxide ion without (**7e**) and with expulsed formaldehyde (**7f**) or methylamine (**7g**). From these results, the effect of the acid catalyst on the transition-state energy is clear. The activation energy of transition states $\mathbf{TS_{7a-1a}}$ is 19.2 kcal mol^{-1}, whereas the activation barrier is raised significantly higher in the presence of hydroxide anion: 28.2 and 31.4 kcal mol^{-1} for $\mathbf{TS_{7e-1d}}$ and $\mathbf{TS_{7f-1e}}$, respectively (Table S2). The effect of a neutral methylamine base is smaller, and it show similar activation energy (21.8 kcal mol^{-1}) to $\mathbf{TS_{7a-1a}}$ for the water-expulsion step. As such, the catalytic effect of the methylammonium ion survives buffered conditions (the presence of methylamine), but it is lost in the presence of a stronger base.

In summary, calculations for the simple formaldehyde oxime models confirm that the reaction pathways of intramolecular oxime transfer reaction contain general acid- or base-catalyzed equilibrium steps that involve synchronous or rapid proton transfers. On the basis of the reaction-energy data, the first two equilibrium steps of the intramolecular oxime transfer reaction can affect the overall reaction rate via the concentration of **7**. However, the water-elimination step, which has the highest transition state and activation energy, most likely plays a more

dx.doi.org/10.1021/jo402676z | *J. Org. Chem.* 2014, 79, 2006–2014

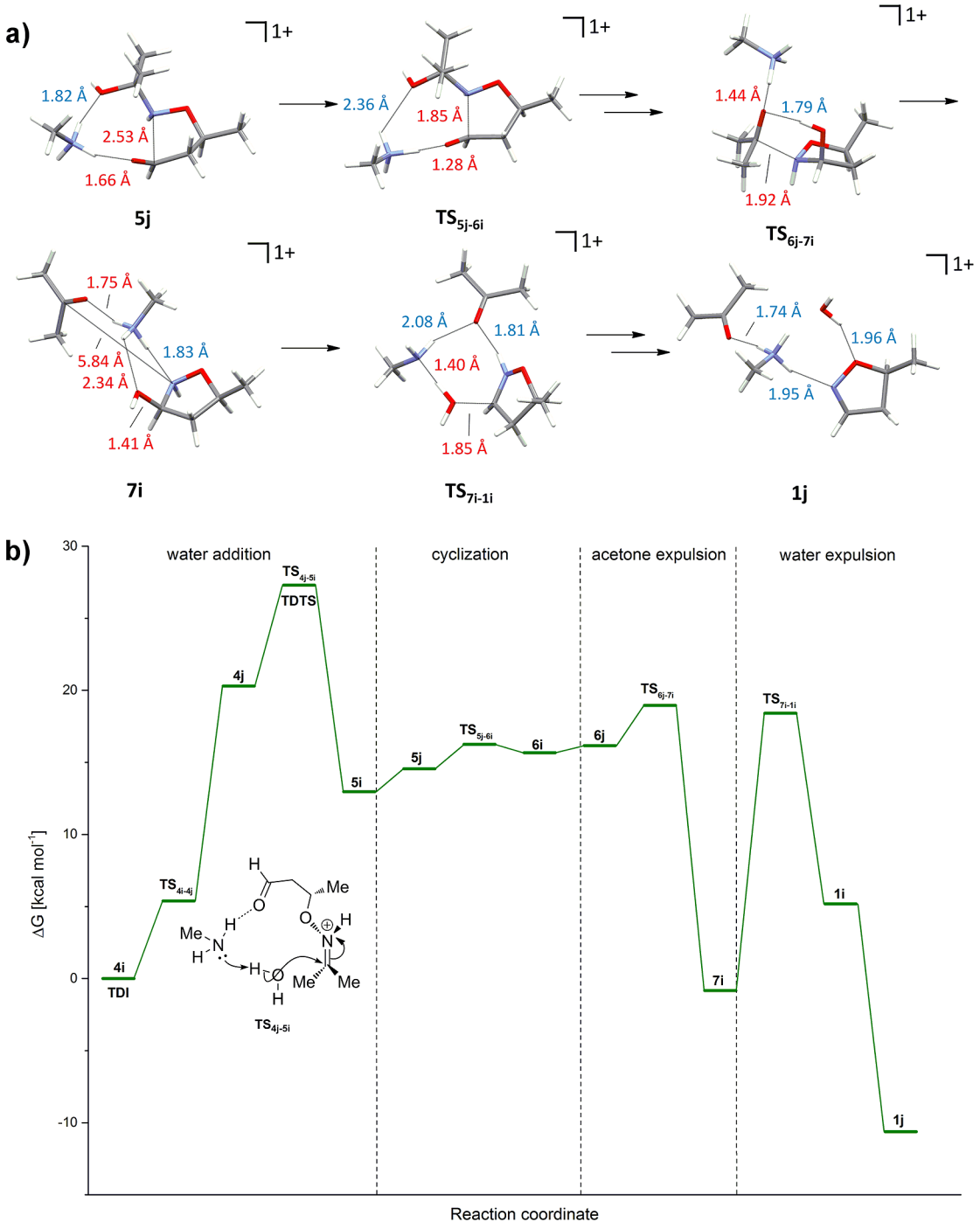

Figure 4. (a) Optimized structures for **5j**, TS_{5j-6i}, TS_{6j-7i}, **7i**, TS_{7i-1i}, and **1j** of the cyclization, acetone-expulsion, and water-expulsion steps of the sequence. The full set of optimized structures is presented in Supporting Information, Figure S6. (b) Calculated Gibbs free energies for the acetone oxime model (for details, see Supporting Information, Table S3). A schematic view of the turnover-determining transition state (TDTS) is presented.

important role in the reaction. It should also be noted that the intermediates and side products of each step have the ability to form different kinds of hydrogen-bonded complexes and small changes in these complexes can alter the reaction-energy profile significantly.

Acetone Oxime Model System. The reaction mechanism of an intramolecular oxime transfer reaction was also investigated in the case of a more realistic system (R^3 = Me and acetone oxime) because this oxime was used in most of the experimental studies.[1] Furthermore, it was still unclear why intermediate **4** is the only species of all of the intermediates that has been observed in experimental studies even though computational studies for the formaldehyde oxime model (R^3 = H) suggest that intermediate **7** might be observable in the reaction mixture because of the considerable activation barrier of the water-expulsion step. To address the question whether the simplicity of the formaldehyde oxime model might have biased the results, calculations of the acetone oxime model were carried out starting from the water-addition step.[17]

dx.doi.org/10.1021/jo402676z | J. Org. Chem. 2014, 79, 2006−2014

The results show that the water-addition step likely takes place via a stepwise mechanism (Figure 3). The first transition state, $\mathbf{TS_{4i-4j}}$, involves two proton-transfer reactions: from methyl ammonium ion to water and from water to nitrogen atom of conjugate addition product **4i**. The second transition state, $\mathbf{TS_{4j-5i}}$, also contains two simultaneous events: the attacking water molecule attaches to the electrophilic carbon atom of **4j** and donates the proton to methylamine at the same time. Even though two different transition states were located for the stepwise mechanism, no intermediate that is lower in energy than transition state $\mathbf{TS_{4i-4j}}$ could be located between transition states $\mathbf{TS_{4i-4j}}$ and $\mathbf{TS_{4j-5i.}}$ Hence, a concerted mechanism was also considered and characterized computationally. In the concerted mechanism, the attacking water molecule donates the proton to the conjugate addition product (Figure 3c). Thus, the methylammonium ion only carriers the positive charge through the step. The concerted reaction pathway has a very high activation barrier (38.8 kcal mol^{-1} higher than $\mathbf{TS_{4i-5i}}$), indicating that the rapid stepwise mechanism is much more likely.

After the water-addition step, the subsequent steps (i.e., the cyclization, expulsion of acetone, and expulsion of water) proceed in a similar manner for both the formaldehyde and acetone oxime model systems and thus they are not discussed anymore in the case of the acetone oxime model (optimized geometries of acetone oxime model are given in Figure S6). Because our computational results for formaldehyde oxime models showed that the effect of different diastereomers on the overall reaction profile was relatively minor, for the last three steps of the reaction, we restrict our discussion only to the first diastereomer series (for **6i,** corresponding to 2*S**,3*R**,5*S** relative stereochemistry) in the case of the acetone oxime model.

As can be seen from Figure 4, of all of the steps of the reaction, the water-addition step has the highest transition state ($\mathbf{TS_{4j-5i}}$) and it also has a high activation energy of ca. 27 kcal mol^{-1}. This result is fully in line with previous computational studies where similar activation barriers were calculated for the addition of water to oximes.[3b] In addition, calculations indicate that conjugate addition product **4i** is clearly lower in energy than reaction product **5i** of the water-addition step, indicating that **4i** is thermodynamically stable. These computational findings readily explain why intermediate **4** can be detected experimentally, and they show that **4i** and $\mathbf{TS_{4j-5i}}$ are the TDI and TDTS, respectively, for the intramolecular oxime transfer reaction. This indicates that the rate of the oxime transfer reaction is mainly controlled by the water-addition step. In our previous experimental studies, we suggested that the final water-expulsion step would involve rate-determining states mainly on the basis of substituent effects observed with β,β-disubstituted enals. However, with simple β-monosubstituted enals (such as the model crotonaldehyde used in this study), the experimentally determined rates of the cyclization depend on the oxime structure in the order cyclohexanone oxime > acetone oxime > cyclopentanone oxime. This order corresponds roughly to the reactivity difference of the corresponding ketones to nucleophilic attack at carbonyl,[18] suggesting that, at least with these oximes, the rate differences in the oxime transfer reaction might indeed be attributed to the rate of the nucleophilic attack.

Our calculations also indicate that the water-expulsion step has a considerable activation barrier (~20.0 kcal mol^{-1}, Figure 4). Although the computational model studied herein predicts the transition state of the water-addition step to be the TDTS, it is conceivable that this picture could change with different substitution patterns in the enal, and both water addition as well as the water-expulsion steps could contribute to the overall rate.[10,19,20] Moreover, the omitted counteranion could also influence the reaction-energy profile, although the relative energies of the intermediates and transition states are likely affected to a lesser extent than the absolute energies. Final product **1j** is much lower in energy (~10 kcal mol^{-1}) than the conjugate addition product, indicating that the intramolecular oxime transfer reaction is clearly exergonic.

CONCLUSIONS

Density functional theory (PBE0/def2-TZVPP) calculations in conjunction with a polarizable continuum model were used to assess the mechanism of the intramolecular oxime transfer reaction and its reaction-energy profile. Although the model compounds employed in the calculations were simplified from the experimental species, the computed activation barrier (27 kcal mol^{-1}) for the oxime transfer reaction is reasonable given the slow rate of the reaction. Moreover, calculations predicted that the formation and decomposition of tetrahedral intermediates (i.e., the addition of water to the oxime carbon or the final expulsion of water to form the isoxazoline) have higher barriers than the remaining steps. These predictions are in line with the experimental evidence obtained for this reaction. Hence, the pathway outlined in this study represents a highly likely pathway for the intramolecular oxime transfer reaction, and the energy profiles obtained computationally present qualitatively correct depictions of the actual energy profiles. However, because the counteranion was omitted from the model and different hydrogen-bonding patterns of the intermediates affect the energies considerably, caution must be exercised in correlating the computed barriers with reaction rates.[21] Nevertheless, this study demonstrates that even complex mechanisms under general acid and base catalysis can be explored via computational methods.

ASSOCIATED CONTENT

Supporting Information

Geometries, Gibbs free energies, electronic energies, and alternative reaction route for the water-expulsion step and *xyz* coordinates of the optimized structures. This material is available free of charge via the Internet at http://pubs.acs.org.

AUTHOR INFORMATION

Corresponding Authors

*E-mail: jani.o.moilanen@jyu.fi (J.M.).
*E-mail: petri.m.pihko@jyu.fi (P.P.).

Notes

The authors declare no competing financial interest.

ACKNOWLEDGMENTS

We thank Drs. Antti Pohjakallio and Heikki Tuononen for valuable discussions and input. Financial support was provided by the University of Jyväskylä, the Academy of Finland (project no. 259532), and the Magnus Ehrnrooth Foundation.

REFERENCES

(1) (a) Pohjakallio, A.; Pihko, P. M. *Chem.—Eur. J.* **2009**, *15*, 3960–3964. (b) Pohjakallio, A.; Pihko, P. M.; Laitinen, U. M. *Chem.—Eur. J.* **2010**, *16*, 11325–11339.

(2) (a) Jencks, W. P. *J. Am. Chem. Soc.* **1959**, *81*, 475−481. (b) More O'Ferrall, R. A.; O'Brien, D. *J. Phys. Org. Chem.* **2004**, *17*, 631−640.
(3) (a) Yamaguchia, Y.; Yasutakeb, N.; Nagaokab, M. *J. Mol. Struct.: THEOCHEM* **2003**, *639*, 137−150. (b) Nsikabaka, S.; Harb, W.; Ruiz-lópez, M. F. *J. Mol. Struct.: THEOCHEM* **2006**, *764*, 161−166. (c) Takahashi, H.; Tanabe, K.; Aketa, M.; Kishi, R.; Furukawa, S.-I.; Nakano, M. *J. Chem. Phys.* **2007**, *126*, 084508−084518. (d) Ronchin, L.; Bortoluzzi, M.; Vavasori, A. *J. Mol. Struct.: THEOCHEM* **2008**, *858*, 46−51.
(4) (a) Rosenberg, S.; Silver, S. M.; Sayer, J. M.; Jencks, W. P. *J. Am. Chem. Soc.* **1974**, *96*, 7986−7998. (b) Sayer, J. M.; Pinsky, B.; Schonbrunn, A.; Washtien, W. *J. Am. Chem. Soc.* **1974**, *96*, 7998−8009.
(5) (a) Perdew, J. P.; Burke, K.; Ernzerhof, M. *Phys. Rev. Lett.* **1996**, *77*, 3865−3868. (b) Perdew, J. P.; Burke, K.; Ernzerhof, M. *Phys. Rev. Lett.* **1997**, *78*, 1396−1396. (c) Perdew, J. P.; Ernzerhof, M.; Burke, K. *J. Chem. Phys.* **1996**, *105*, 9982−9985.
(6) Weigenda, F.; Ahlrichs, R. *Phys. Chem. Chem. Phys.* **2005**, *7*, 3297−3305.
(7) (a) Miertuš, S.; Scrocco, E.; Tomasi, J. *Chem. Phys.* **1981**, *55*, 117−129. (b) Miertuš, S.; Tomasi, J. *Chem. Phys.* **1982**, *65*, 239−245. (c) Pascual-Ahuir, J. L.; Silla, E.; Tuñón, I. *J. Comput. Chem.* **1994**, *15*, 1127−1138. (d) Cossi, M.; Barone, V.; Cammi, R.; Tomasi, J. *Chem. Phys. Lett.* **1996**, *255*, 327−335. (e) Barone, V.; Cossi, M.; Tomasi, J. *J. Chem. Phys.* **1997**, *107*, 3210−3221. (f) Cancès, E.; Mennucci, B.; Tomasi, J. *J. Chem. Phys.* **1997**, *107*, 3032−3041. (g) Mennucci, B.; Tomasi, J. *J. Chem. Phys.* **1997**, *106*, 5151−5158. (h) Mennucci, B.; Cancès, E.; Tomasi, J. *J. Phys. Chem. B* **1997**, *101*, 10506−10517. (i) Tomasi, J.; Mennucci, B.; Cancès, E. *J. Mol. Struct.: THEOCHEM* **1999**, *464*, 211−226. (j) Tomasi, J.; Mennucci, B.; Cammi, R. *Chem. Rev.* **2005**, *105*, 2999−3093.
(8) (a) Fukui, K. *Acc. Chem. Res.* **1981**, *14*, 363−368. (b) Hratchian, H. P.; Schlegel, H. B. *J. Chem. Phys.* **2004**, *120*, 9918−9924. (c) Hratchian, H. P.; Schlegel, H. B. In *Theory and Applications of Computational Chemistry: The First Forty Years*; Dykstra, C. E., Frenking, G., Kim, K. S., Scuseria, G., Eds.; Elsevier: Amsterdam, The Netherlands, 2005; pp 195−249. (d) Hratchian, H. P.; Schlegel, H. B. *J. Chem. Theory Comput.* **2005**, *1*, 61−69.
(9) Frisch, M. J.; Trucks, G. W.; Schlegel, H. B.; Scuseria, G. E.; Robb, M. A.; Cheeseman, J. R.; Scalmani, G.; Barone, V.; Mennucci, B.; Petersson, G. A.; Nakatsuji, H.; Caricato, M.; Li, X.; Hratchian, H. P.; Izmaylov, A. F.; Bloino, J.; Zheng, G.; Sonnenberg, J. L.; Hada, M.; Ehara, M.; Toyota, K.; Fukuda, R.; Hasegawa, J.; Ishida, M.; Nakajima, T.; Honda, Y.; Kitao, O.; Nakai, H.; Vreven, T.; Montgomery, J. A., Jr.; Peralta, J. E.; Ogliaro, F.; Bearpark, M.; Heyd, J. J.; Brothers, E.; Kudin, K. N.; Staroverov, V. N.; Kobayashi, R.; Normand, J.; Raghavachari, K.; Rendell, A.; Burant, J. C.; Iyengar, S. S.; Tomasi, J.; Cossi, M.; Rega, N.; Millam, J. M.; Klene, M.; Knox, J. E.; Cross, J. B.; Bakken, V.; Adamo, C.; Jaramillo, J.; Gomperts, R.; Stratmann, R. E.; Yazyev, O.; Austin, A. J.; Cammi, R.; Pomelli, C.; Ochterski, J. W.; Martin, R. L.; Morokuma, K.; Zakrzewski, V. G.; Voth, G. A.; Salvador, P.; Dannenberg, J. J.; Dapprich, S.; Daniels, A. D.; Farkas, O.; Foresman, J. B.; Ortiz, J. V.; Cioslowski, J.; Fox, D. J. *Gaussian 09*, revision C.01; Gaussian, Inc.: Wallingford, CT, 2009.
(10) (a) Kozuch, S.; Amatore, C.; Jutand, A.; Shaik, S. *Organometallics* **2005**, *24*, 2319−2330. (b) Kozuch, S.; Shaik, S. *Acc. Chem. Res.* **2011**, *44*, 101−110.
(11) Macrae, C. F.; Bruno, I. J.; Chisholm, J. A.; Edgington, P. R.; McCabe, P.; Pidcock, E.; Rodriguez-Monge, L.; Taylor, R.; van de Streek, J.; Wood, P. A. *J. Appl. Crystallogr.* **2008**, *41*, 466−470.
(12) For some examples, see: (a) Ilieva, S.; Galabov, B.; Musaev, D. G.; Morokuma, K.; Schaefer, H. F. *J. Org. Chem.* **2003**, *68*, 1496−1502. (b) Jin, L.; Wang, W.; Hua, D.; Lü, J. *Phys. Chem. Chem. Phys.* **2013**, *15*, 9034−9042. (c) Schreiner, E.; Nair, N. N.; Marx, D. *J. Am. Chem. Soc.* **2009**, *131*, 13668−13675. (d) Wang, Y.-N.; Topol, I. A.; Collins, J. R.; Burt, S. K. *J. Am. Chem. Soc.* **2003**, *125*, 13265−13273. (e) Pasalić, H.; Aquino, A. L.; Tunega, D.; Haberhauer, G.; Gerzabek, M. H.; Georg, H. C.; Moraes, T.; Coutinho, K.; Canuto, S.; Lischka, H. *J. Comput. Chem.* **2010**, *31*, 2046−2055. (f) Kuznetsov, M. L.; Kukushkin, V. Y. *J. Org. Chem.* **2006**, *71*, 582−592. (g) Carzía Ruano, J. L.; Clemente, F. R.; González Gutiérrez, L.; Gordillo, R.; Martín Castro, A. M.; Rodríguez Ramos, J. H. *J. Org. Chem.* **2002**, *67*, 2926−2933.
(13) PBE0 is able to describe hydrogen bonds with a good accuracy. For some examples, see: (a) Zhao, Y.; Truhlar, D. G *J. Chem. Theory Comput.* **2005**, *1*, 415−432. (b) Johnson, E. R.; DiLabio, G. A. *Chem. Phys. Lett.* **2006**, *419*, 333−339. (c) Santra, B.; Michaelides, A.; Scheffler, M. *J. Chem. Phys.* **2007**, *127*, 184104-1−184104-9. (d) Campo, J. M.; Gázquez, J. L.; Trickey, S. B.; Vela, A. *J. Chem. Phys.* **2012**, *136*, 104108-1−104108-8.
(14) The diastereomers are assigned as follows: **6a** (first diastereomer series): (2*R**,3*R**,5*S**), **6a′** (second diastereomer series): (2*R**,3*R**,5*R**), **6a″** (third diastereomer series): (2*R**,3*S**,5*S**), and **6a‴** (fourth diastereomer series): (2*R**,3*S**,5*R**).
(15) For the water-expulsion step, we also investigated an alternative reaction route in which protonated formaldehyde acts as an acid catalysis instead of methylammonium ion. However, this route is more unlikely than the reaction route presented in the Figure 1 (for more details, see the Supporting Information).
(16) The free energies of **6a**−**6a‴** were used to calculate the activation energies of the aldehyde-expulsion step because they are starting materials for the aldehyde-expulsion step and are lower in energy than **6b**−**6b‴**.
(17) It is a well-known fact that different substituents affect reaction energies; for some examples, see: (a) Calzadilla, M.; Malpica, A.; Cordova, T. *J. Phys. Org. Chem.* **1999**, *12*, 708−712. (b) Gajewski, J. J. *J. Am. Chem. Soc.* **1979**, *101*, 4393−4394. (c) Yoo, H. Y.; Houk, K. N. *J. Am. Chem. Soc.* **1997**, *119*, 2877−2884. (d) Tian, J.; Houk, K. N.; Klärner, F. G. *J. Phys. Chem. A* **1998**, *102*, 7662−7667.
(18) (a) Finiels, A.; Geneste, P. *J. Org. Chem.* **1979**, *44*, 1577. For a discussion of the reactivity difference between cyclohexanones and cyclopentanones, see: (b) Brown, H. C.; Brewster, J. H.; Shechter, H. *J. Am. Chem. Soc.* **1954**, *76*, 467−474.
(19) It has been proven that in multistep reactions several steps/states play an important role in determining an overall reaction rate. For some examples, see: (a) Murdoch, J. R. *J. Chem. Educ.* **1981**, *58*, 32−36. (b) Fey, N. *Dalton Trans.* **2010**, *39*, 296−310. (c) Sparta, M.; Børve, K. J.; Jensen, V. R. *J. Am. Chem. Soc.* **2007**, *129*, 8487−8499. (d) Zuidema, E.; Escorihuela, L.; Eichelsheim, T.; Carbó, J. J.; Bo, C.; Kamer, P. C. J.; van Leeuwen, P. W. N. M. *Chem.—Eur. J.* **2008**, *14*, 1843−1853.
(20) For an example of an earlier study where the computational and experimental methods can predict different steps for the rate-determining step, see ref 17d.
(21) It should also be noted that the inclusion of the expulsed acetone in calculations lowers the free energy of $\mathbf{TS}_{7i-1i}$ considerably because of the hydrogen-bonded network. If the free energy of the transition state is calculated without expulsed acetone and then scaled to fit reaction energy data, then $\mathbf{TS}_{7i-1i}$ is 2.5 kcal mol^{-1} higher in energy.